RSC Advances

PAPER

View Article Online
View Journal | View Issue

Cite this: *RSC Adv.*, 2015, **5**, 83648

Incorporation of cisplatin into the metal–organic frameworks UiO66-NH_2 and UiO66 – encapsulation *vs.* conjugation

Katarzyna A. Mocniak,[a] Ilona Kubajewska,[b] Dominic E. M. Spillane,[c] Gareth R. Williams[b] and Russell E. Morris*[a]

This work demonstrates synthetic strategies for the incorporation of an anticancer drug, cisplatin, and a Pt(IV) cisplatin prodrug into two zirconium-based metal–organic-frameworks (MOFs): UiO66 and UiO66-NH_2. Cisplatin was chosen due to its reported high potency in killing *ca.* 95% of different cancers. Two approaches for its incorporation were investigated: conjugation and encapsulation. In the conjugation route, a Pt(IV) cisplatin prodrug was incorporated into UiO66-NH_2 utilising its amine group in an amide-coupling reaction. In the second case, cisplatin was encapsulated into the large cavities of both MOFs. The presence of platinum was confirmed by energy-dispersive X-ray spectroscopy and microwave plasma-atomic emission spectroscopy. The cytotoxicity of the formulations was assessed on the A549 lung cancer cell line. The results show that the system in which cisplatin is conjugated to UiO66-NH_2 is more efficient in inducing cell death than the materials where cisplatin is encapsulated into the pores of the MOFs. This is consistent with the higher drug loading achieved with the conjugation technique. One disadvantage of cisplatin therapy is that it may lead to thrombosis and, as a consequence, to heart attack and cardiac arrest. To ameliorate this potential side effect, we investigated the incorporation of NO (which has been widely researched for its antithrombotic properties) into the drug-loaded MOFs. All the cisplatin or pro-drug loaded MOFs are able to entrap and then release NO. Furthermore, the amount of NO released from these formulations is much greater than from the pure MOFs. As a result, the drug delivery systems developed in this work have potentially potent double functionality.

Received 16th July 2015
Accepted 25th September 2015

DOI: 10.1039/c5ra14011k

www.rsc.org/advances

Introduction

Cancer is one of the most feared diseases known to mankind. Therefore, the development of new and more efficient drugs has continuously attracted a great deal of attention. There are a number of known anticancer drugs targeting different metabolic pathways, such as alkylating agents (busulfan, melphalan, chlorambucil), anti-metabolites (asparaginase, 5-fluorouracil, methotrexate) or DNA linking agents (carboplatin, cisplatin or oxoplatin). Cisplatin, *cis*-[$Pt(NH_3)_2Cl_2$], is the most commonly used and researched drug for a variety of cancers. Despite its high toxicity (due to being a first generation drug), cisplatin is used in the treatment of head, neck, ovarian, cervical, testicle, breast and bladder tumours.[1] The toxicity of cisplatin against cancerous cells was first recognized in 1968.[2] Over subsequent years of intensive research, it showed high efficacy against many cancer types in clinical trials[3] and was finally approved as an anti-tumour drug by the FDA (Food and Drug Administration) in 1978.[4] Cisplatin is capable of forming intra- and inter-strand cross-links with nucleic acids of DNA. This leads to cell death (apoptosis) due to the resultant inability of DNA to replicate.[5]

It must be noted that cisplatin does not act very specifically, and affects all cells as it cannot distinguish between cancerous and healthy cells. Even though its clinical effectiveness is relatively high, it comes with many side-effects including nephrotoxicity and neurotoxicity, together with possible development of drug resistance over time. Many trials have targeted the synthesis of so-called "warheads" that can target the unique metabolic pathways of tumour cells (such as the glucose-based respiration that causes them to offer a reductive environment[6]), thereby increasing specificity. Non-toxic Pt(IV) species can be activated into Pt(II) antitumour agents *in vivo* by reducing agents such as glutathione.[1b,7,14b,22] Thus, Pt(IV) based compounds can be successfully used as cisplatin prodrugs. An example of such a Pt(IV) complex is satraplatin, which can be orally administered and becomes active after reduction by ascorbate and glutathione (GSH) in the malignant cells.[8]

Another approach to circumvent the shortcomings of cisplatin is through targeted drug delivery systems.[1b,9] A variety

[a]*School of Chemistry, University of St Andrews, North Haugh, St Andrews, KY16 9ST, UK. E-mail: rem1@st-andrews.ac.uk; Tel: +44 (0)1334 463818*

[b]*UCL School of Pharmacy, University College London, 29–39 Brunswick Square, WC1N 1AX, London, UK*

[c]*School of Human Sciences, London Metropolitan University, 166-220 Holloway Road, N7 8DB, London, UK*

of systems have been designed to release the drug only inside a tumour cell, and to leave healthy cells untouched. Carbon nanotubes,[10] liposomes,[1b,11] polymers[1b,12] and nano-sized metal phosphates[1a] or oxides[13] are all under investigation as suitable drug carriers. In addition to these systems, metal–organic frameworks (MOFs) have recently come to the fore as drug delivery systems, and may potentially be of use in cancer therapy.[14]

MOFs are a comparatively new class of materials: they were first synthesised by Robson in 1989.[15] They offer great potential in many applications, for example CO_2 capture and hydrogen storage,[16] gas separation and purification,[17] heterogeneous catalysis,[18] luminescence,[19] MRI imaging[20] and biomedicine.[21] MOFs are porous materials with tunable surface areas and a wide range of pore sizes.[22] Methods exploiting their adsorption capacities for drug storage and delivery are hence of increasing interest.[23] In this work, two biocompatible MOFs based on Zr and 1,4-benzenedicarboxylate building blocks, UiO66 (Fig. 1) and UiO66-NH_2, were employed as cisplatin delivery devices.

In addition to the problems of non-specificity identified above, anticancer therapy using cisplatin may lead to thrombosis:[24] the formation of blood clotting that may cause hypoxia and in extreme cases tissue death, heart attacks and strokes. Entrapment of nitric oxide (NO) – known for its anti-thrombosis, anti-inflammatory and anti-bacterial effects[14b,25] – in the cisplatin-loaded MOFs, could mitigate this risk. Previous studies have shown that NO can be stored and released on demand by the MOFs HKUST-1, CPO-27-Mg and CPO-27-Ni.[26] Nitric oxide itself has also been reported to cause cancer cell death.[27] Thus, preparing MOFs loaded with both cisplatin and NO should permit the production of dual-functionality systems without compromising the anticancer efficacy of the former.

In this work we examined whether we could successfully encapsulate cisplatin in the UiO66 $[Zr_6O_4(OH)_4BDC]_6$ (BDC = 1,4-benzenedicarboxylate see Fig. 1) and UiO66-NH_2 $[Zr_6O_4(OH)_4(BDC\text{-}NH_2)_6]$ (BDC-NH_2 = 2-amino-1,4-benzenedicarboxylate) MOFs, utilising their pores. Both UiO66 and UiO66-NH_2 have very high porosities, offering octahedral (11 Å radius) and tetrahedral (8 Å radius) cages[28,29] that could accommodate cisplatin, which is *ca.* 5 Å in size.[30] UiO66 and UiO66-NH_2 have the same basic structure, but the latter has a free amine group on the organic linker. This means that while both systems can take cisplatin up into their pores, UiO66-NH_2 can also potentially form covalent bonds with a guest through this amine group. For the latter, we used a platinum prodrug with a carboxylic group, *cis*,*cis*,*trans*-$[Pt^{IV}(NH_3)_2Cl_2(O_2CCH_2CH_2CO_2H)(OH)]$ (Fig. 2), and UiO66-NH_2. The idea was to conjugate the Pt(IV) prodrug to UiO66-NH_2 by covalent bonds similar to peptide bonds.

The major aim of our study was to determine which of these approaches – encapsulation or conjugation – is more efficient for drug delivery. To ameliorate some of the common side effects of cisplatin therapy, bifunctional systems loaded with nitric oxide were also prepared. We believe this study sheds more light on using MOFs as drug delivery systems and specifically their potential supportive roles in cancer treatments.

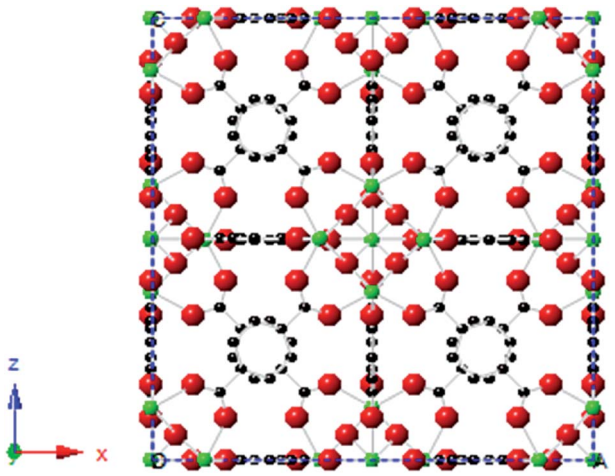

Fig. 1 The crystal structure of UiO66, based on CCSD deposition file 733458. Zr (green), O (red) and C (black) are represented by coloured spheres.

Experimental section

All materials for MOF synthesis and cisplatin, *cis*-$[Pt(NH_3)_2Cl_2]$, were obtained from Sigma Aldrich and used without further purification. UiO66, UiO66-NH_2 and *cis*,*cis*,*trans*-$[Pt^{IV}(NH_3)_2(Cl)_2(O_2CCH_2CH_2CO_2H)(OH)]$ were prepared according to literature procedures.[31]

MOF synthesis

UiO66. A mixture of zirconium(IV) chloride (82 mg, 0.35 mmol) and 1,4-benzenedicarboxylic acid (58 mg, 0.35 mmol) in dimethyl formamide (DMF; 5 mL) was acidified using HCl (37 wt%, 805 μL, 9.7 mmol) and acetic acid (concentrated, 605 μL, 10.57 mmol). The solution was sealed inside a 23 mL Teflon-lined steel autoclave and heated at 220 °C under autogenous pressure for 24 hours. The UiO66 product was collected by vacuum filtration, washed with DMF and dried in vacuum. Yield: 117 mg, 84%.

UiO66-NH_2. A mixture of zirconium(IV) chloride (82 mg, 0.35 mmol) and 2-amino-1,4-benzenedicarboxylic acid (63 mg, 0.35 mmol) in DMF (5 mL) was acidified using HCl (37 wt%, 805 μL 9.7 mmol) and acetic acid (concentrated, 605 μL, 10.57 mmol). The solution was sealed inside a 23 mL Teflon-lined steel autoclave and heated at 120 °C under autogenous pressure for 24 hours. The UiO66-NH_2 product was collected by

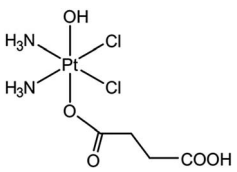

Fig. 2 The structure of the cisplatin prodrug used in this work.

vacuum filtration, washed with DMF and dried in vacuum. Yield: 130 mg, 90%.

Encapsulation method

For this method both MOFs (UiO66 and UiO66-NH_2) were used. The procedure was as follows: MOF powders (*ca.* 350 mg) were dehydrated under dynamic vacuum overnight and then immersed in a solution of cisplatin, *cis*-[$Pt(NH_3)_2Cl_2$], (35 mL, at 80% of saturation solubility, 2 mg mL^{-1}, (6.66 mM) in deionised water). This corresponded to a theoretical loading of 29.8 mg of cisplatin per 100 mg of dehydrated MOF. The encapsulation continued for 48 hours under stirring at room temperature. The samples were centrifuged and allowed to dry in air.

Prodrug synthesis

A prodrug of cisplatin, *cis*,*cis*,*trans*-[$Pt^{IV}(NH_3)_2(Cl)_2(O_2CCH_2CH_2CO_2H)(OH)$] (see Fig. 2), was synthesised in the following procedure. A suspension of cisplatin (0.4 g, 1.33 mmol) in H_2O (12 mL) at 60 °C was oxidized with H_2O_2 (20 mL) added dropwise. The reaction was left for 4 h, and the resultant bright yellow solution left to cool overnight. Yellow crystals (yield: 234 mg, 53%) were recovered by filtration and washed with ice cold water. A more detailed procedure can be found in the literature.[7a,32] The product (202 mg, 0.6 mol) was then reacted with succinic anhydride (60 mg, 0.6 mol) at 70 °C in a DMF (5 mL) suspension for 24 h and then cooled to room temperature. DMF was removed under vacuum and the residual suspension (1 mL) was dissolved in acetone, and a pale yellow solid precipitated with diethyl ether. Yield: 180 mg, 70%.

Incorporation of the prodrug into UiO66-NH_2 (conjugation method)

The prodrug (Fig. 2) was conjugated to UiO66-NH_2 using the EDC/NHS method in an aqueous solution. A detailed procedure can be found in the literature.[11b,33] In brief, 1-ethyl-3-(3-dimethylaminopropyl)carbodiimide (EDC·HCl 0.038 g, 0.20 mmol) and *N*-hydroxysuccinimide (NHS 0.023 g, 0.20 mmol) were dissolved in de-ionized water (15 mL) under stirring. Next, the prodrug (0.70 g, 0.16 mmol) was added into the aqueous solution. After the solution became clear, MOF UiO66-NH_2 (0.140 g) was added and the reaction mixture stirred at room temperature for 24 h. Finally, the solid product was recovered by vacuum filtration, washed with water and left to dry in air. Elemental analysis of the prodrug: calculated: [C] = 11.06%, [H] = 2.76%, [O] = 6.45%, found: [C] = 10.75, [H] = 2.67%, [O] = 6.45%.

Nitric oxide loading

In order to activate (remove solvent from) the MOF powders (0.015 g per glass vial), they were first placed under vacuum (2.3×10^{-3} bar) during which time *ca.* 30% of the mass was lost. They were then heated to 120 °C while still under dynamic vacuum and held at this temperature overnight, leaving a fully activated material. The samples were subsequently cooled to room temperature and exposed to *ca.* 2 atm of dry NO (99.5%, Air Liquide) for 45 min. The vials were next evacuated and exposed to dry argon, before being flame sealed. This cycle of evacuation and argon flushing was repeated three times in order to remove any residual physisorbed NO from the surfaces of the MOF and glassware.

Drug release experiments

The drug-loaded UiO66-NH_2 and UiO66 powders were formulated into pellets using a hand press in order ensure reproducibility in the drug release experiments. The pellets contained 25 wt% of the drug-loaded MOF, with the remaining 75% being Teflon. In each experiment, two pellets of 20 mg each, were added to 10 mL of a pH 7.4 TRIS buffer (prepared from 100 mL 0.1 M TRIS, 84 mL 0.1 M HCl, and 12 mL deionised H_2O) at 37 °C. Aliquots of 0.5 mL were removed after the following times: 15 min, 30 min, 1 h, 2 h, 3 h, 4 h, 5 h, 24 h. Cisplatin release was quantified in terms of the amounts of Pt in solution, using an Agilent MP4100 microwave plasma-atomic emission spectrometer (MP-AES). Experiments were performed in duplicate. All calculations for the extent of release are related to the amount of active powder in a pellet.

Cell culture

The A549 lung cancer cell line (ATCC) was stimulated for 24 h with the MOF formulations. The growth media used for cell culture was Gibco RPMI 1640 supplemented with penicillin (100 μg mL^{-1}), streptomycin (100 μg mL^{-1}), L-glutamine (292 μg mL^{-1}) (all Life Technologies) and 10% v/v heat-inactivated fetal bovine serum (FBS; Gibco). This is henceforth referred to as "complete RMPI". Cells were incubated at 37 °C (5% CO_2) and passaged in this medium until required for stimulation.

For the latter, 2% FBS in complete RPMI was used for cell seeding. Cells were harvested with the TrypLE Express Enzyme (1×; Life Technologies) and seeded at a concentration of 40 000 cells per mL in a 96-well flat bottomed plate, with 100 μL of cell suspension added to each well. Suspensions of the MOF formulations were prepared with a concentration of 1 mg/100 μL and aliquots of 10, 30 and 50 μL were used to stimulate the cells. Complete RPMI was added to even up the volume in wells to 150 μL over the plate. This corresponded to 100 μg, 300 μg and 500 μg of MOF per well respectively. A cisplatin solution was prepared as a positive control, with a concentration of 1 mg mL^{-1} (3.33 mM). The aliquots used for cell stimulations were the same as those for MOF powders: 10 μL (222 μM), 30 μL (666 μM) and 50 μL (1110 μM).

The Alamar Blue cell viability assay was used to evaluate cell viability after 24 h exposure to the MOFs. Resazurin solution (5 mM in RPMI) was added at 10% of the well volume (15 μL to 150 μL well volume), and incubated for 4 h. The fluorescence of each well was quantified using a SpectraMax Multi-Mode Microplate reader (Molecular Devices) with excitation/emission wavelengths set at 555/585 nm. After 4 hours, a linear relationship between fluorescence intensity and cell number was observed. The standard curve was constructed as follows: fluorescence of untreated cells corresponded to 100% viability and 0% cells (RPMI media alone) to 0% viability, with additional calibration points at 75%, 50% and 25%.

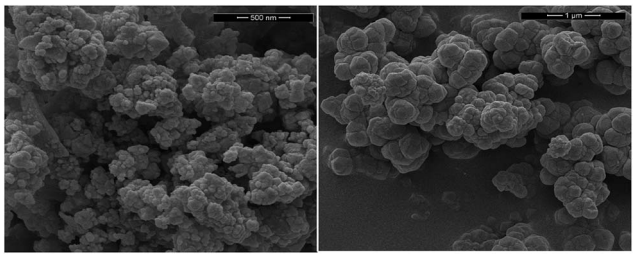

Fig. 3 SEM images of UiO66-NH_2 (left) and UiO66 (right).

Material characterization and instrumentation

Powder X-ray diffraction (PXRD) patterns were collected on a PANalytical Empyrean diffractometer using Cu Kα radiation. Scanning electron microscopy-energy dispersive X-ray spectroscopy (SEM-EDX) was performed on a JEOL JSM-5600 instrument at a 20 keV excitation energy. Thermogravimetric analysis (TGA) was conducted on a Discovery instrument (TA Instruments) using approximately 2–3 mg of the sample, which was heated at 10 °C min^{-1} to 800 °C under a flow of N_2 gas (25 mL min^{-1}). IR spectra were recorded over the region of 600–4000 cm^{-1} on a Shimadzu ATR spectrophotometer.

NO release measurements were performed using a Sievers NOA 280i chemiluminescence analyzer. Calibration of the instrument was performed by passing air through a zero filter (Sievers < 1 ppb NO) and 91 ppm NO gas (AP, balance nitrogen). The flow rate was set to 200 mL min^{-1} with a cell pressure of 8.5 Torr and an oxygen pressure of 6.1 psi. In order to trigger and measure the NO release, dry nitrogen gas was humidified by passing it over a solution of LiCl (sat.) to give 11% R.H.

Results and discussion

Encapsulation of cisplatin in the pores of UiO66-NH_2 and UiO66

Successful preparation of the MOFs was confirmed by X-ray diffraction, with the patterns of the obtained materials being identical to those reported in the literature. The particle size of the MOFs was assessed by SEM to be around 500–600 nm (Fig. 3). EDX quantification indicates that the cisplatin loading is 4.7 wt% and 4.9 wt% for UiO66 and UiO66-NH_2 respectively. Pt : Zr ratios are shown in Table 1. The dose of cisplatin typically used in anti-cancer therapy is 20 mg m^{-2} per day for 5 days in the case of testicular cancer and 75–100 mg m^{-2} administered every 4 weeks for ovarian cancer.[34] An average male of 175 cm weighing 80 kg has a body surface area of 1.99 m^2 (according to the Boyd formula[35]). Applying the same formula to an average female of 165 cm weighing 58 kg results in 1.63 m^2. This would mean that in order to use the MOFs loaded with cisplatin in these therapies an amount of *ca.* 2.4–3.2 g would be necessary to treat ovarian cancer, or approx. 0.8 g for testicular cancer, if 100% of the encapsulated cytotoxic material was released.

Table 1 Cisplatin loading calculated based on EDX analysis

MOF	Pt : Zr ratio (mol)	Corresponding to cisplatin loading wt%
UiO66-NH_2-prodrug	1.00 : 1.76	30.7
UiO66-NH_2 encapsulated	1.00 : 15.91	4.9
UiO66 encapsulated	1.00 : 17.38	4.7

Conjugation of the prodrug to the amine group of UiO66-NH_2

The amide-coupling reaction allows for the direct incorporation of a non-toxic Pt(IV) prodrug to the MOF using its amine group. The Pt(IV) prodrug can be easily reduced in the oxygen-poor environment typical of tumour cells to give cytotoxic Pt(II) species. The UiO66-NH_2 integrity was retained after the prodrug loading process: this is clear from the powder X-ray diffraction data in Fig. 4, where the pattern is observed to be unchanged post-incorporation. Attempts were made to reduce the Pt(IV) prodrug with ascorbic acid[7a] and quantify the amount of cisplatin released by ^{195}Pt NMR, but the signal to noise ratio was low and the results therefore inconclusive. However, EDX analysis clearly demonstrates pro-drug conjugation (see Table 1). These data show that the ratio of Pt : Zr in the prodrug-conjugated UiO66-NH_2 is 1 : 1.76, which corresponds to 30.7 wt% loading (expressed w.r.t cisplatin) and indicates that approximately every second amine group has successfully been functionalised with the pro-drug. EDX mapping is shown in Fig. 5. Pt and Zr are in the same areas of the image, indicating the presence of a drug in the pores of the UiO66-NH_2.

Infrared spectroscopy (Fig. 6) shows bands at around 1580 and 1730 cm^{-1} corresponding to amide groups, proving a peptide bond is formed between the Pt(IV) prodrug and the amine group in UiO66-NH_2. Small bands corresponding to amine groups can also be seen, as not all available amine groups on the MOF were involved in the conjugation. The band at 1750 in the MOF, completely disappeared after conjugation, which can serve as a proof of a successful conjugation.

TGA was performed in order to assess the thermal stability of the formulations. The data suggest that the MOF with a conjugated cisplatin prodrug is not as thermally stable as the unmodified UiO66-NH_2, and starts decomposing at 300 °C, (50 °C lower than unmodified UiO66-NH_2; Fig. 7).

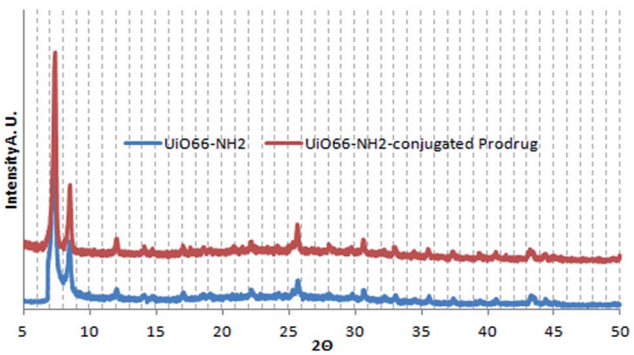

Fig. 4 Powder X-ray diffraction patterns of UiO66-NH_2, before (blue) and after (red) conjugation with a cisplatin prodrug. Plots are shifted vertically for clarity.

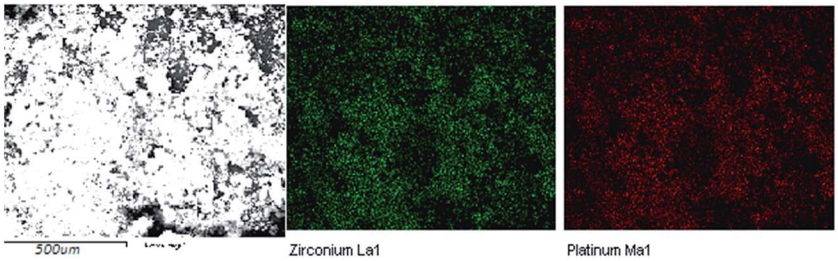

Fig. 5 EDX mapping of UiO66-NH_2 conjugated with the prodrug. Left: The SEM image of the studied area; centre and right: elemental mapping of Pt and Zr by EDX. Red and green markings denote Pt and Zr, respectively.

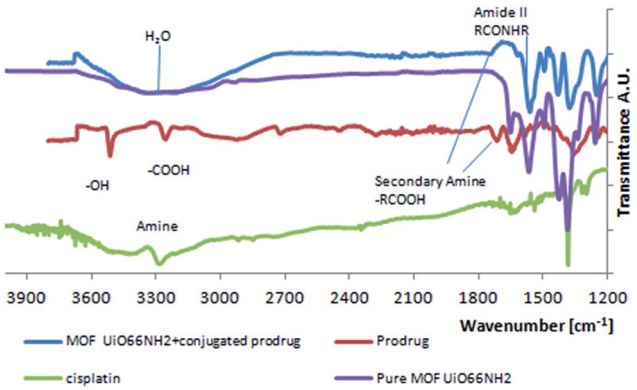

Fig. 6 IR spectra of UiO66-NH_2 before and after conjugation, together with those of the prodrug and cisplatin. Spectra are vertically shifted for clarity.

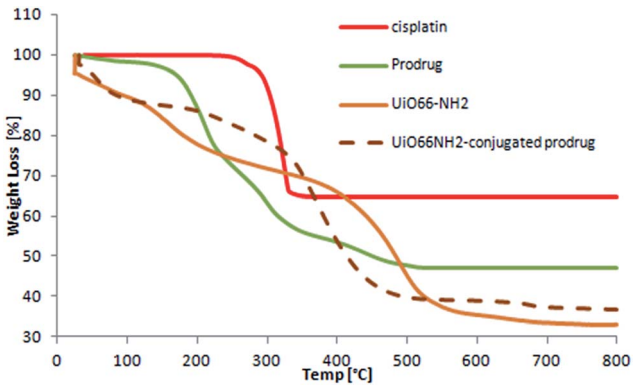

Fig. 7 Thermogravimetric analysis data for the materials explored in this work.

Drug release. Cisplatin release data are given in Fig. 8. UiO66 releases 22.73 μg of cisplatin per mg of MOF in the first 24 hours, approximately four times more than the amount released from UiO66-NH_2 (5.88 μg cisplatin per mg MOF). However, the EDX analysis shows that the cisplatin loading is similar in both MOFs (4.9 wt% in UiO66-NH_2 and 4.7 wt% in UiO66). The results possibly indicate a relatively strong interaction between cisplatin and the amine group in UiO66-NH_2 MOF, preventing release of the former. As a result, after 24 h only 12.5% of loaded cisplatin in the active MOF powder is being released in the case of UiO66-NH_2 while in UiO66 the release amount is 48%.

Cell viability studies

The lung cancer cell line A549 was stimulated with different MOF formulations and cell viability was examined after 24 h exposure using the Alamar Blue assay. This cell line was selected for *in vitro* studies because cisplatin is commonly used to treat lung cancer. The data are presented as mean ± SEM (standard error of the mean) from two independent experiments, with each set of conditions run in triplicate in each experiment. Statistical analysis was performed by Repeated Measures ANOVA and Sidak's multiple comparisons test using GraphPad Prism v6.05 software. Differences between means were considered statistically significant when $P < 0.05$ (*), $P < 0.01$ (**), $P < 0.001$ (***), or $P < 0.0001$ (****). "*P*" is the probability of obtaining the observed effect purely due to chance. $P < 0.05$ is the conventional threshold for a statistically significant result, and indicates that there is only a 5% of chance that the conclusion drawn is in fact false. Subsequent levels of significance commonly used in statistics are $P < 0.01$, $P < 0.001$, $P < 0.0001$, which denote 1%, 0.1% and 0.01% chance, respectively. The lower the *P* value obtained, the higher the level of significance of the observed effect and, consequently, the greater our confidence that it is true.

Fig. 9(a) shows the viability of cancer cells in response to UiO66 and UiO66-NH_2 encapsulated with cisplatin at three different concentrations. We observed that cisplatin loaded UiO66 significantly decreased cell viability compared to UiO66 alone. Conversely, the analogous UiO66-NH_2 systems did not induce significant changes in cell viability. This may be due to the fact that cisplatin bind to amine groups in the MOF, and is thus not available for release and interaction with cells. These findings agree with the results from cisplatin release (discussion *vide supra*).

In Fig. 9(b), we compared the cytotoxic efficacy of UiO66-NH_2 with encapsulated cisplatin and UiO66-NH_2 conjugated with the cisplatin prodrug. It appears that the latter performed better in inducing cell death, particularly at higher concentrations where statistically significant outcomes were observed. This is expected to be a result of the higher drug loading in the conjugated system, as well as the binding between cisplatin and the amide groups of UiO66-NH_2. The conjugated UiO66-NH_2 system shows approximately the same cytotoxicity as the encapsulated UiO66

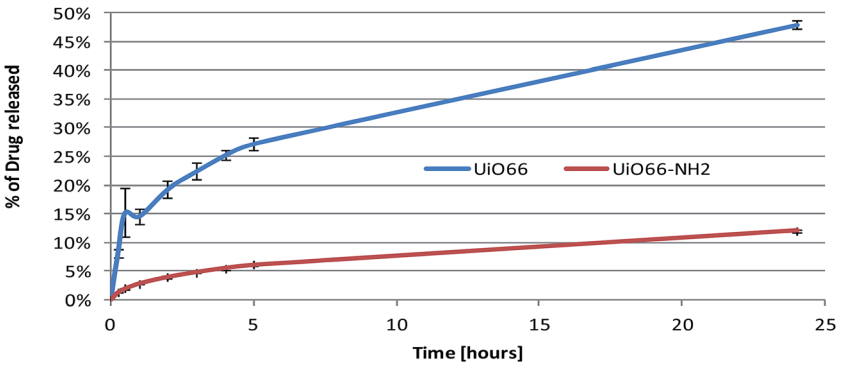

Fig. 8 Cisplatin release from UiO66 (violet) and UiO66-NH_2 (red) pellets in TRIS buffer. The results of two independent experiments are shown as mean ± SEM.

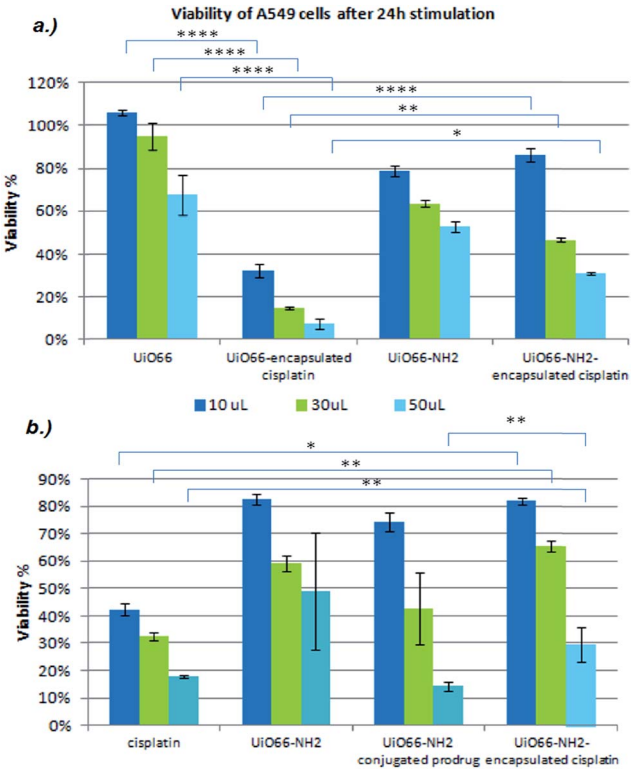

Fig. 9 Cell viability after 24 h exposure to the MOF systems: (a) UiO66 and UiO66-NH_2 with and without encapsulated cisplatin; (b) UiO66-NH_2 with encapsulated cisplatin and conjugated with the prodrug. Results are from two separate experiments, each of them conducted in triplicate, and are shown as mean ± SEM.

at higher concentrations, but is less effective at low concentrations. This can be ascribed to the fact that the UiO66-encapsulated cisplatin is freely able to exit the MOF, while for the prodrug to be active hydrolysis of the amide linkage is required. This makes the conjugated system require more time to become active, but offers promise for sustained release and selectivity for cancerous cells only.

In all cases we observe a distinct dose-dependent effect of the drug-loaded MOFs on cell viability. It is clear that these systems are biologically functional, and thus have potential as drug delivery systems.

Nitric oxide adsorption

While UiO66 and UiO66-NH_2 have high pore volumes, they do not have any open metal sites with which to effectively bind nitric oxide, and in the two systems only the amine group in UiO66-NH_2 can perform this function. The amine group has in this work been utilized for conjugation with the prodrug to form a peptide bond. Nevertheless, cisplatin and the prodrug themselves offer open sites on their amine groups and Pt centres.

NO-loading and NO release from the untreated MOFs and all three drug-loaded materials were performed in triplicate. The release profiles are depicted in Fig. 10 and the absolute quantities of NO involved are summarized in Table 2. The incorporation of cisplatin into the pores of the UiO66 material significantly increased the amount of NO loaded and released from the system, since the cisplatin complex offers two amine groups and a metal site to which NO can bind.

The unmodified UiO66-NH_2 shows more NO release than UiO66 due to the presence of NH_2 groups, which can form the diazeniumdiolate group (NONOate)[36] with NO. Again, the encapsulation of cisplatin leads to a dramatic increase in NO release capability. The amount of NO released is nearly 1500 times higher for UiO66 and *ca.* 3 times greater for UiO66-NH_2 after cisplatin encapsulation. We may thus assume that in cisplatin loaded systems, nitric oxide can be coordinated to the Pt and amine groups of cisplatin as well as to amine groups of the organic linker in the case of UiO66-NH_2. Note that the levels of NO released are well above those required for anti-platelet activation (anti-thrombosis) activity.[37]

In contrast, when UiO66-NH_2 is conjugated with the cisplatin prodrug there is almost no change in NO release performance. This is thought to be because: (i) although the introduction of the prodrug provides additional amine groups, it also occupies the NH_2 groups of the MOF, and (ii) the bulky nature of the prodrug complex (see Fig. 1) may present steric hindrance for the coordination of NO molecules to its amine groups, reducing the ability of incoming NO to bind to them.

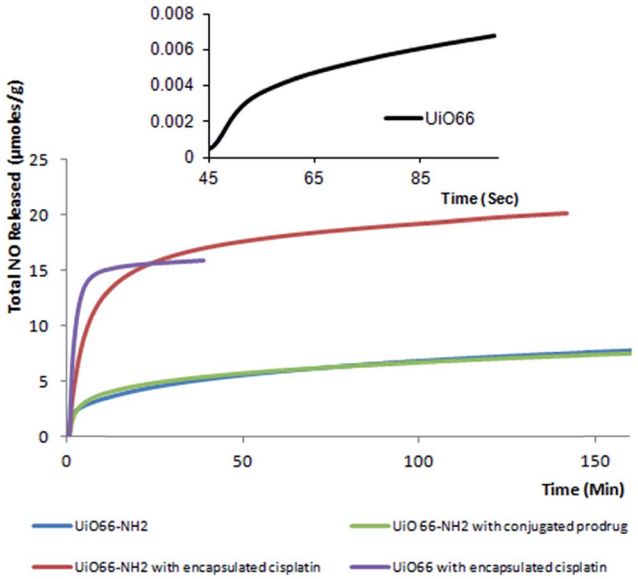

Fig. 10 Total NO release from UiO66-NH_2 (blue), UiO66-NH_2 conjugated with the prodrug (green), and with cisplatin encapsulated (red), and from UiO66 loaded with cisplatin (purple). Inset: NO release from pure UiO66.

Table 2 Amounts of nitric oxide released from the MOFs, shown as mean ± SEM

MOF	Total NO (µmoles per g of MOF)
UiO66	$11.3 \times 10^{-3} \pm 1.87$
UiO66-NH_2	9.27 ± 3.95
UiO66-prodrug (conjugated)	7.69 ± 0.43
UiO66-cisplatin (encapsulated)	16.5 ± 4.25
UiO66-NH_2-cisplatin (encapsulated)	22.7 ± 5.53

Conclusions

Using a solvothermal method, in this work we first synthesized the MOFs UiO66 and UiO66-NH_2. We next loaded them with cisplatin using two approaches – encapsulation of cisplatin to both MOFs and conjugation of a cisplatin prodrug to UiO66-NH_2. The prodrug investigated, *cis*,*cis*,*trans*-[$Pt^{IV}(NH_3)_2(Cl)_2(O_2CCH_2CH_2CO_2H)(OH)$] is expected to allow the selective targeting of tumour cells because it is only reduced to an active Pt(II) species under the highly reducing conditions typical of such cells. The results obtained show that for UiO66-NH_2 conjugation allows higher loading than encapsulation (30.7 wt% against 4.9 wt%), and that this translates into greater cytotoxicity in an *in vitro* assay. Considering the encapsulated systems, the amount of release of cisplatin from UiO66 is significantly higher than from UiO66-NH_2, even though EDX results suggest that the drug loading is similar in both systems. This may be due to an interaction of cisplatin with amine groups of the UiO66-NH_2 MOF.

In addition, the cisplatin loaded MOFs were successfully loaded with NO, with the aim of preventing the thrombotic effects that can occur with cisplatin therapy. Nitric oxide release is unaffected by the conjugation of the prodrug to UiO66-NH_2. However, MOFs loaded with cisplatin present much higher NO release capacities than the pure materials, due to the open sites available for NO binding on cisplatin.

To conclude, our results demonstrate a successful approach for the synthesis of a bifunctional material containing Pt-based anticancer agents and nitric oxide as both an antitumour and antithrombotic agent.

Acknowledgements

The authors wish to thank the EPSRC (EP/K005499/1 and EP/K025112/1) and the British Heart Foundation (NH/11/8/29253) for funding. We thank Mr David McCarthy UCL School of Pharmacy for SEM images.

References

1 (*a*) A. Diaz, M. L. Gonzalez, R. J. Perez, A. David, A. Mukherjee, A. Baez, A. Clearfield and J. L. Colon, Direct intercalation of cisplatin into zirconium phosphate nanoplatelets for potential cancer nanotherapy, *Nanoscale*, 2013, **5**, 11456–11463; (*b*) H. Xiao, L. Yan, Y. Zhang, R. Qi, W. Li, R. Wang, S. Liu, Y. Huang, Y. Li and X. Jing, A dual-targeting hybrid platinum(IV) prodrug for enhancing efficacy, *Chem. Commun.*, 2012, **48**, 10730–10732; (*c*) R. Wang, H. Xiao, H. Song, Y. Zhang, X. Hu, Z. Xie, Y. Huang, X. Jing and Y. Li, Co-delivery of all-*trans*-retinoic-acid and cisplatin(IV) prodrug based on polymer-drug conjugates for enhanced efficacy and safety, *J. Mater. Chem.*, 2012, **22**, 25453–25462.

2 M. H. Greene, Is cisplatin a human carcinogen?, *J. Natl. Cancer Inst.*, 1992, **84**, 306–312.

3 O. Rixe, W. Ortuzar, M. Alvarez, R. Parker, E. Reed, K. Paull and T. Fojo, Oxaliplatin, tetraplatin, cisplatin, and carboplatin: spectrum of activity in drug-resistant cell lines and in the cell lines of the national cancer institute's anticancer drug screen panel, *Biochem. Pharmacol.*, 1996, **52**, 1855–1865.

4 E. R. Jamieson and S. J. Lippard, Structure, Recognition, and Processing of Cisplatin–DNA Adducts, *Chem. Rev.*, 1999, **99**, 2467–2498.

5 W. H. Ang, S. Pilet, R. Scopelliti, F. Bussy, L. Juillerat-Jeanneret and P. J. Dyson, Synthesis and Characterization of Platinum(IV) Anticancer Drugs with Functionalized Aromatic Carboxylate Ligands: Influence of the Ligands on Drug Efficacies and Uptake, *J. Med. Chem.*, 2005, **48**, 8060–8069.

6 S. Dhar and S. J. Lippard, Mitaplatin, a potent fusion of cisplatin and the orphan drug dichloroacetate, *Proc. Natl. Acad. Sci. U. S. A.*, 2009, **106**, 22199–22204.

7 (*a*) Y. Shi, S.-A. Liu, D. J. Kerwood, J. Goodisman and J. C. Dabrowiak, Pt(IV) complexes as prodrugs for cisplatin, *J. Inorg. Biochem.*, 2012, **107**, 6–14; (*b*) B. Ahn, J. Park,

K. Singha, H. Park and W. J. Kim, Mesoporous silica nanoparticle-based cisplatin prodrug delivery and anticancer effect under reductive cellular environment, *J. Mater. Chem. B*, 2013, **1**, 2829–2836.

8 D. Gibson, The mechanism of action of platinum anticancer agents-what do we really know about it?, *Dalton Trans.*, 2009, **48**, 10681–10689.

9 (*a*) V. Pinzani, F. Bressolle, I. Johanne Haug, M. Galtier, J. Blayac and P. Balmès, Cisplatin-induced renal toxicity and toxicity-modulating strategies: a review, *Cancer Chemother. Pharmacol.*, 1994, **35**, 1–9; (*b*) Z. H. Siddik, D. R. Newell, F. E. Boxall and K. R. Harrap, The comparative pharmacokinetics of carboplatin and cisplatin in mice and rats, *Biochem. Pharmacol.*, 1987, **36**, 1925–1932.

10 A. H. Tamsyn and M. H. James, Modelling the encapsulation of the anticancer drug cisplatin into carbon nanotubes, *Nanotechnology*, 2007, **18**, 275704.

11 (*a*) J. Yang, W. Mao, M. Sui, J. Tang and Y. Shen, Platinum(IV)-coordinate polymers for cancer drug delivery, *J. Controlled Release*, 2011, **152**, E108–E109; (*b*) H. Song, H. Xiao, Y. Zhang, H. Cai, R. Wang, Y. Zheng, Y. Huang, Y. Li, Z. Xie, T. Liu and X. Jing, Multifunctional Pt(IV) pro-drug and its micellar platform: to kill two birds with one stone, *J. Mater. Chem. B*, 2013, **1**, 762–772; (*c*) A. Samad, Y. Sultana and M. Aqil, Liposomal Drug Delivery Systems: An Update Review, *Curr. Drug Delivery*, 2007, **4**, 297–305; (*d*) E. A. Leite, C. M. Souza, A. D. Carvalho-Junior, L. G. V. Coelho, A. M. Q. Lana, G. D. Cassali and M. C. Oliveira, Encapsulation of cisplatin in long-circulating and pH-sensitive liposomes improves its antitumour effect and reduces acute toxicity, *Int. J. Nanomed.*, 2012, **7**, 5259–5269.

12 H. Xiao, R. Qi, S. Liu, X. Hu, T. Duan, Y. Zheng, Y. Huang and X. Jing, Biodegradable polymer – cisplatin(IV) conjugate as a pro-drug of cisplatin(II), *Biomaterials*, 2011, **32**, 7732–7739.

13 S. V. Devi and T. Prakash, Kinetics of Cisplatin Release by *In vitro* Using Poly(D,L-Lactide) Coated Fe_3O_4 Nanocarriers, *IEEE Transactions on NanoBioscience*, 2013, **12**, 60–63.

14 (*a*) C.-Y. Sun, C. Qin, X.-L. Wang and Z.-M. Su, Metal–organic frameworks as potential drug delivery systems, *Expert Opin. Drug Delivery*, 2013, **10**, 89–101; (*b*) A. C. McKinlay, R. E. Morris, P. Horcajada, G. Ferey, R. Gref, P. Couvreur and C. Serre, BioMOFs: metal–organic frameworks for biological and medical applications, *Angew. Chem., Int. Ed. Engl.*, 2010, **49**, 6260–6266; (*c*) W. J. Rieter, K. M. Pott, K. M. L. Taylor and W. Lin, Nanoscale Coordination Polymers for Platinum-Based Anticancer Drug Delivery, *J. Am. Chem. Soc.*, 2008, **130**, 11584–11585.

15 B. F. Hoskins and R. Robson, Infinite polymeric frameworks consisting of three dimensionally linked rod-like segments, *J. Am. Chem. Soc.*, 1989, **111**, 5962–5964.

16 (*a*) K. Sumida, D. L. Rogow, J. A. Mason, T. M. McDonald, E. D. Bloch, Z. R. Herm, T.-H. Bae and J. R. Long, Carbon Dioxide Capture in Metal–Organic Frameworks, *Chem. Rev.*, 2011, **112**, 724–781; (*b*) K. M. Thomas, Adsorption and desorption of hydrogen on metal–organic framework materials for storage applications: comparison with other nanoporous materials, *Dalton Trans.*, 2009, 1487–1505; (*c*) P. D. C. Dietzel, V. Besikiotis and R. Blom, Application of metal–organic frameworks with coordinatively unsaturated metal sites in storage and separation of methane and carbon dioxide, *J. Mater. Chem.*, 2009, **19**, 7362–7370; (*d*) K. L. Mulfort and J. T. Hupp, Chemical reduction of metal–organic framework materials as a method to enhance gas uptake and binding, *J. Am. Chem. Soc.*, 2007, **129**, 9604–9605; (*e*) D. Zhao, D. Yuan and H.-C. Zhou, The current status of hydrogen storage in metal–organic frameworks, *Energy Environ. Sci.*, 2008, **1**(2), 222–235; (*f*) S. Ma and H.-C. Zhou, Gas storage in porous metal–organic frameworks for clean energy applications, *Chem. Commun.*, 2010, **46**(1), 44–53; (*g*) L. J. Murray, M. Dinca and J. R. Long, Hydrogen storage in metal–organic frameworks, *Chem. Soc. Rev.*, 2009, **38**, 1294–1314.

17 J.-R. Li, J. Sculley and H.-C. Zhou, Metal–Organic Frameworks for Separations, *Chem. Rev.*, 2011, **112**, 869–932.

18 (*a*) J. Lee, O. K. Farha, J. Roberts, K. A. Scheidt, S. T. Nguyen and J. T. Hupp, Metal–organic framework materials as catalysts, *Chem. Soc. Rev.*, 2009, **38**, 1450–1459; (*b*) A. Henschel, K. Gedrich, R. Kraehnert and S. Kaskel, Catalytic properties of MIL-101, *Chem. Commun.*, 2008, 4192–4194; (*c*) A. Corma, H. García and F. X. Llabrés i Xamena, Engineering Metal Organic Frameworks for Heterogeneous Catalysis, *Chem. Rev.*, 2010, **110**, 4606–4655.

19 M. D. Allendorf, C. A. Bauer, R. K. Bhakta and R. J. T. Houk, Luminescent metal–organic frameworks, *Chem. Soc. Rev.*, 2009, **38**, 1330–1352.

20 (*a*) M. Kurmoo, Magnetic metal–organic frameworks, *Chem. Soc. Rev.*, 2009, **38**(5), 1353–1379; (*b*) K. M. L. Taylor, W. J. Rieter and W. Lin, Manganese-Based Nanoscale Metal–Organic Frameworks for Magnetic Resonance Imaging, *J. Am. Chem. Soc.*, 2008, **130**, 14358–14359; (*c*) K. M. L. Taylor-Pashow, J. D. Rocca, Z. Xie, S. Tran and W. Lin, Postsynthetic Modifications of Iron-Carboxylate Nanoscale Metal–Organic Frameworks for Imaging and Drug Delivery, *J. Am. Chem. Soc.*, 2009, **131**, 14261–14263.

21 (*a*) R. E. Morris and P. S. Wheatley, Gas storage in nanoporous materials, *Angew. Chem., Int. Ed.*, 2008, **47**, 4966–4981; (*b*) P. K. Allan, P. S. Wheatley, D. Aldous, M. I. Mohideen, C. Tang, J. A. Hriljac, I. L. Megson, K. W. Chapman, G. De Weireld, S. Vaesen and R. E. Morris, Metal–organic frameworks for the storage and delivery of biologically active hydrogen sulfide, *Dalton Trans.*, 2012, **41**, 4060–4066; (*c*) P. Horcajada, R. Gref, T. Baati, P. K. Allan, G. Maurin, P. Couvreur, G. Ferey, R. E. Morris and C. Serre, Metal–Organic Frameworks in Biomedicine, *Chem. Rev.*, 2012, **112**, 1232–1268; (*d*) R. C. Huxford, J. Della Rocca and W. Lin, Metal–organic frameworks as potential drug carriers, *Curr. Opin. Chem. Biol.*, 2010, **14**(2), 262–268; (*e*) P. Horcajada, C. Serre, M. Vallet-Regí, M. Sebban, F. Taulelle and G. Férey, Metal–Organic Frameworks as Efficient Materials for Drug Delivery, *Angew. Chem.*, 2006, **118**, 5974–5978.

22 (*a*) C.-D. Wu and W. Lin, Highly Porous, Homochiral Metal–Organic Frameworks: Solvent-Exchange-Induced Single-

Crystal to Single-Crystal Transformations, *Angew. Chem., Int. Ed.*, 2005, **44**, 1958–1961; (*b*) P. Horcajada, F. Salles, S. Wuttke, T. Devic, D. Heurtaux, G. Maurin, A. Vimont, M. Daturi, O. David, E. Magnier, N. Stock, Y. Filinchuk, D. Popov, C. Riekel, G. Férey and C. Serre, How Linker's Modification Controls Swelling Properties of Highly Flexible Iron(III) Dicarboxylates MIL-88, *J. Am. Chem. Soc.*, 2011, **133**, 17839–17847.

23 (*a*) S. Keskin and S. Kizilel, Biomedical Applications of Metal Organic Frameworks, *Ind. Eng. Chem. Res.*, 2011, **50**, 1799–1812; (*b*) P. Horcajada, T. Chalati, C. Serre, B. Gillet, C. Sebrie, T. Baati, J. F. Eubank, D. Heurtaux, P. Clayette, C. Kreuz, J. S. Chang, Y. K. Hwang, V. Marsaud, P. N. Bories, L. Cynober, S. Gil, G. Ferey, P. Couvreur and R. Gref, Porous metal–organic-framework nanoscale carriers as a potential platform for drug delivery and imaging, *Nat. Mater.*, 2010, **9**(2), 172–178; (*c*) D. Farrusseng, *Metal-Organic Frameworks: Applications from Catalysis and Gas Storage*, Wiley-VCH Verlag GmbH & Co. KGaA, 2011.

24 (*a*) T. Proverbs-Singh, S. K. Chiu, Z. Liu, S. Seng, G. Sonpavde, T. K. Choueiri, C.-K. Tsao, M. Yu, N. M. Hahn, W. K. Oh and M. D. Galsky, Arterial Thromboembolism in Cancer Patients Treated With Cisplatin: A Systematic Review and Meta-analysis, *J. Natl. Cancer Inst.*, 2012, **104**, 1837–1840; (*b*) M. Jafri and A. Protheroe, Cisplatin-associated thrombosis, *Anti-Cancer Drugs*, 2008, **19**, 927–929; (*c*) D. D. Fernandes, M. L. Louzada, C. A. Souza and F. Matzinger, Acute aortic thrombosis in patients receiving cisplatin-based chemotherapy, *Curr. Oncol.*, 2011, **18**, e97–e100.

25 (*a*) S. Huerta, S. Chilka and B. Bonavida, Nitric oxide donors: novel cancer therapeutics (review), *Int. J. Oncol.*, 2008, **33**, 909–927; (*b*) N. J. Hinks, A. C. McKinlay, B. Xiao, P. S. Wheatley and R. E. Morris, Metal organic frameworks as NO delivery materials for biological applications, *Microporous Mesoporous Mater.*, 2010, **129**, 330–334.

26 (*a*) F. Bonino, S. Chavan, J. G. Vitillo, E. Groppo, G. Agostini, C. Lamberti, P. D. C. Dietzel, C. Prestipino and S. Bordiga, Local Structure of CPO-27-Ni Metallorganic Framework upon Dehydration and Coordination of NO, *Chem. Mater.*, 2008, **20**, 4957–4968; (*b*) A. C. McKinlay, B. Xiao, D. S. Wragg, P. S. Wheatley, I. L. Megson and R. E. Morris, Exceptional behavior over the whole adsorption-storage-delivery cycle for NO in porous metal organic frameworks, *J. Am. Chem. Soc.*, 2008, **130**, 10440–10444; (*c*) E. Garrone, B. Fubini, E. Escalona Platero and A. Zecchina, Thermodynamic characterization of the adsorption of nitric oxide at the {100} face of nickel monoxide microcrystals, *Langmuir*, 1989, **5**, 240–245.

27 S. Duan, S. Cai, Q. Yang and M. L. Forrest, Multi-arm polymeric nanocarrier as a nitric oxide delivery platform for chemotherapy of head and neck squamous cell carcinoma, *Biomaterials*, 2012, **33**, 3243–3253.

28 X. Zhu, J. Gu, Y. Wang, B. Li, Y. Li, W. Zhao and J. Shi, Inherent anchorages in UiO-66 nanoparticles for efficient capture of alendronate and its mediated release, *Chem. Commun.*, 2014, **50**, 8779–8782.

29 F. Jeremias, V. Lozan, S. K. Henninger and C. Janiak, Programming MOFs for water sorption: amino-functionalized MIL-125 and UiO-66 for heat transformation and heat storage applications, *Dalton Trans.*, 2013, **42**, 15967–15973.

30 T. A. Hilder and J. M. Hill, Modelling the encapsulation of the anticancer drug cisplatin into carbon nanotubes, *Nanotechnology*, 2007, **18**, 275704.

31 M. J. Katz, Z. J. Brown, Y. J. Colon, P. W. Siu, K. A. Scheidt, R. Q. Snurr, J. T. Hupp and O. K. Farha, A facile synthesis of UiO-66, UiO-67 and their derivatives, *Chem. Commun.*, 2013, **49**, 9449–9451.

32 M. Reithofer, M. Galanski, A. Roller and B. K. Keppler, An Entry to Novel Platinum Complexes: Carboxylation of Dihydroxoplatinum(IV) Complexes with Succinic Anhydride and Subsequent Derivatization, *Eur. J. Inorg. Chem.*, 2006, 2612–2617.

33 S. Dhar, W. L. Daniel, D. A. Giljohann, C. A. Mirkin and S. J. Lippard, Polyvalent Oligonucleotide Gold Nanoparticle Conjugates as Delivery Vehicles for Platinum(IV) Warheads, *J. Am. Chem. Soc.*, 2009, **131**, 14652–14653.

34 http://Drugs.com is the most popular, comprehensive and up-to-date source of drug information online. Providing free, peer-reviewed, accurate and independent data on more than 24 000 prescription drugs, over-the-counter medicines & natural products.

35 http://cancerguide.org/drugdosing.htmL, WWW Source.

36 A. Lowe, P. Chittajallu, Q. Gong, J. Li and K. J. Balkus Jr, Storage and delivery of nitric oxide *via* diazeniumdiolated metal organic framework, *Microporous Mesoporous Mater.*, 2013, **181**, 17–22.

37 B. Xiao, P. S. Wheatley, X. Zhao, A. J. Fletcher, S. Fox, A. G. Rossi, I. L. Megson, S. Bordiga, L. Regli, K. M. Thomas and R. E. Morris, High-Capacity Hydrogen and Nitric Oxide Adsorption and Storage in a Metal–Organic Framework, *J. Am. Chem. Soc.*, 2007, **129**, 1203–1209.